CHAPTER IX.G

SELECTIVITY FOR THE CONVERSION OF SYNGAS

Included in the targeted goals was the attainment of 88% (CO + H_2) conversion at a CO conversion of 90%. At the high CO conversion level of 90%, even an unpromoted iron catalyst gave less than 88% (CO + H_2) conversion. Thus, we were never successful in obtaining the target conversion for (CO + H_2) using a single pass process. As shown in Figure IX.G-1, at some level of CO conversion the hydrogen conversion becomes equal to the CO conversion and we designated this the "equivalence point." For CO conversions below the equivalence point, hydrogen conversion is greater than that of CO, and at CO conversions above the equivalence point the CO conversion is greater than that of hydrogen. Thus, we can readily define from this type of plot whether it is possible to attain the targeted 88% (CO + H_2) conversion.

Kölbel and Ralek (IX.G-1) reported 90% CO conversion and a conversion of (CO + H_2) of 88%. The values in reference IX.G-1 were apparently taken from reference IX.G-2 where the authors refer to single pass reactor operation as well as recycle operation. Based upon our data (Figure IX.G-1), to obtain 88% (CO + H_2) conversion at 90% CO conversion requires the use of either recycle or multiple reactors.

Kölbel and coworkers (IX.G-1, IX.G-2) report that their yield of C_1 plus C_2 corresponds to 11 or 12 g/Nm^3 with respect to the added CO + H_2. However, as this appears in the German, it does not appear possible to decide whether this value is based upon the (CO + H_2) that is converted or that is fed. The amount of total

hydrocarbons produced (176 or 178 g/Nm^3) suggest that the yield data refer to syngas fed; even if this is the case, the yield of hydrocarbons is only about 200 g/Nm^3 for each Nm^3 of syngas that is converted. This production of hydrocarbons is low. For example Mobil reported values of 207 to 220 gHC/Nm^3 (CO + H_2) converted (ref. IX.G-3) and this is in line with what we obtain in our studies. It is not readily apparent why the hydrocarbon yield that is reported by Kölbel and coworkers is so low. In any event, the hydrocarbon yield obtained repeatedly in our work has greatly exceeded the target value of 178 g/Nm^3 and has been greater than 200 g/Nm^3 for all of the catalysts with higher activities.

The target value for methane plus ethane and ethene was 12 g/Nm^3. This value corresponds to 6.74 percent of the 178 g of total hydrocarbon that was produced in the work of Kölbel and coworkers (IX.G-1,IX.G-2) which served as our targeted value. This value has not been obtained to date for any of our runs that have been conducted at 270°C. In our run where the space velocity was varied, the methane plus ethane weight fraction of the total hydrocarbons increased with increasing CO conversion (Figure IX.G-2). Thus, at low conversion the methane plus ethane corresponded to less than 10 wt.% of the hydrocarbon products but increased to greater than 15 wt.% at the 90% CO conversion level. On the basis of obtaining low methane plus ethane production, it appears desirable to conduct the synthesis either using recycle or to use a series of reactors, keeping the conversion reasonably low in each reactor.

The alkene selectivity does not vary appreciably with alkali loading in the 0.1 to 0.5 wt.% range. Thus, a typical plot of the fraction of alkene for each carbon number

is illustrated in Figure IX.G-3. It is seen that the maximum amount of alkene (minimum alkane) occurs in the C_4-C_5 range. The use of ^{14}C-tracers permitted us to show that the increase in alkane fraction for carbon numbers greater than C_4-C_5 was predominantly due to longer residence time in the reactor which permitted a longer time for secondary reactions (IX.G-4). On the other hand, the addition of labeled ethene showed that the reason for the high fraction of alkane that was produced below the C_4-C_5 range was that competitive adsorption and subsequent hydrogenation was more rapid than for the higher carbon number alkenes. In general, the curve shown in Figure IX.G-3 is representative of all of the alkene distributions that we have obtained. For a typical catalyst containing 0.5 wt.% K and operating at 270°C and 175 psig, the C_5-C_{12} carbon number product fraction contains 65-70% alkenes.

The question of a two (or more) alpha plot for the Anderson-Schulz-Flory plot has a long history. Some of this history is summarized below.

The Fischer-Tropsch Synthesis may be viewed as a simple polymerization reaction, the monomer being CO or a C_1 species derived from it. Schulz (IX.G-5,IX.G-6) derived an equation for the distribution of molecular weights of polymers obtained by a free radical polymerization process, that is, through a one-by-one addition of monomer to a growing chain. The Schulz distribution function is applicable generally if there is a **constant** probability of chain growth, α, and $\alpha < 1$; the latter requirement applies when some reaction limits the chain growth. The probability for chain growth, α, is defined as:

$$\alpha = r_P/(r_P + \Sigma r_t) \qquad [1]$$

where r_P is the rate of chain propagation and r_t is the rate of chain transfer or chain termination. The probability of the chain growth step to take place P times without termination is

$$P_p = \alpha_1 \alpha_2 \alpha_3 \ldots \alpha_p = \alpha^P \quad [2]$$

The number of molecules per degree of polymerization P, n_p, is proportional to the probability of their formation

$$n_p = const\ \alpha^P \quad [3]$$

The mass fraction m_p is proportional to n_p as well as the molecular weight of the components of the fraction ($M_p = M_M P$, where M_M is the molecular weight of the monomer)

$$m_p = AP\alpha^P \quad [4]$$

where A contains the constant M_M. The mass fraction is defined so that

$$\Sigma m_p = 1 \quad [5]$$

The mass fraction is considered to be a continuous function so that

$$\int_o^\infty m_p dP = A\int_o^\infty P\alpha^P dP = 1 \quad [6]$$

and

$$A = 1/\int_o^\infty P\alpha^P dP \quad [7]$$

Solving the integral ($\alpha < 1$, $\alpha^\infty = 0$) and combining equations [4] and [7] leads to

$$m_p = (ln^2\alpha)P\alpha^P \quad [8]$$

Rearranging gives the more familiar form

$$\log(m_p/P) = \log(ln^2\alpha) + (\log\ \alpha)P \quad [9]$$

Thus, a plot of log (m_p/P) versus P should result in a straight line.

Flory published a number of theoretical distribution functions for this and other types of macromolecular formation (e.g., reference IX.G-7). Thus, polymer scientists usually designate distributions as represented by eq. [9] as conforming to a Schulz-Flory distribution.

Similar equations were derived, apparently independently, by catalysis scientists (IX.G-8 - IX.G-10). Anderson continued his efforts to develop chain growth mechanisms and to account for the products formed by chain branching (IX.G-11). Many catalysis scientists therefore recognize Anderson's contributions to the Fischer-Tropsch Synthesis by designating equation [9], and plots based upon it, as an Anderson-Schulz-Flory (ASF) equation or plot, and we shall follow this practice.

Anderson (IX.G-12) summarized product distribution results up to about 1954. Included in this review were the results of the Schwarzheide tests using catalysts from Lurgi, Brabag, K.W.I., I.G. Farben, Ruhrchemie, and Rheinpreussen as well as tests at the larger U.S. pilot plants, and Standard Oil Co. of New Jersey (Figure IX.G-4). These results included operations with iron catalysts both in fixed and fluidized reactors. The results in Figure IX.G-4 clearly indicate that a single α value does not adequately describe the data. Up to carbon number 9 to 11 the data fit one alpha value for equation [9] very well; however, a second α value is needed to describe

those products higher than carbon number 9 to 11. These early workers did not have the benefit of gas chromatography to analyze the higher molecular weight products. Thus, while Anderson noted the need for two or more alpha values to describe the products from FTS using iron catalysts, it received little attention. Furthermore, FTS products from a cobalt catalyst were adequately described with a single alpha value.

Madon and Taylor (IX.G-13) conducted extensive tests with a precipitated, alkali-promoted iron-copper catalyst. They reported a product distribution for the condensed products from FTS using a plug flow reactor that exhibited a two-alpha plot (Figure IX.G-5) but the break occurred at a higher carbon number than those in Figure IX.G-4. Madon and Taylor (IX.G-13) noted that Anderson and coworkers (IX.G-14) had obtained such a plot but with the break occurring at a lower carbon number. Madon and Taylor noted that Hall et al. (IX.G-15) had suggested that in addition to stepwise growth with a single carbon intermediate, multiple build-in of growing chains could occur and that this could affect the growth rate of heavy hydrocarbons. Madon and Taylor, after considering this explanation, suggested instead that chain growth takes place on at least two types of sites, each having a slightly different chain growth probability α.

Novak et al. (IX.G-16) considered the impact of readsorption of α-olefins upon the products from a continuous stirred tank reactor (CSTR) and a plug flow reactor (PFR). They also considered that α-olefins could only initiate chain growth, or that they can also isomerize to internal olefins as well as be hydrogenated. For the CSTR, these authors concluded that, even with such secondary reactions, the products still exhibit an ASF plot. For the PFR, the products deviate from an ASF plot when α-

olefins can undergo only chain initiation. If, however, as is the case in a more realistic situation, the α-olefin also undergoes hydrogenation and isomerization in addition to chain initiation, the distribution rapidly becomes similar to an ASF distribution. Finally, these authors considered the case where the chain growth parameter was allowed to vary along the length of a PFR by forcing the C_1 surface concentration to vary and found, in this case also, that the distribution is quite close to a Flory distribution.

Satterfield and Huff (IX.G-17) initially concluded that the products for a doubly promoted catalyst (C-73, United Catalysts, Inc.) in a CSTR yielded a precise linear relationship between the log of the mole fraction of the products and the carbon number as predicted by an ASF distribution provided all products, including oxygenate species, were included. The linear relationship held over four orders of magnitude of the moles of products and for carbon numbers from 1 to about 20 over a wide range of gas compositions. The chain growth probability factor, α, increased slightly from 0.67 at 269°C to 0.71 at 234°C.

Huff and Satterfield (IX.G-18), after re-examination of their previous data and a consideration of new experimental data on three different iron catalysts, reported that in some cases, the ASF distribution plot can only be well represented by two straight lines with a marked break occurring at about C_{10}. However, when the products are considered on the basis of compound classes, the situation shown in Figure IX.G-4 is an oversimplification. As shown in Figure IX.G-6, Huff and Satterfield found that only the paraffins deviate from the ASF plot; oxygenates and alkenes appear to follow a single ASF plot with $\alpha \sim 0.55$.

Egiebor et al. (IX.G-19) also reported that the break in the ASF plot was due to the alkanes. These authors showed that α-olefins and cis- and trans-β-olefins all show straight line plots with different slopes. They concluded that all these compounds are primary products. The fact that only paraffins show a break in the ASF slope proves that paraffins are not secondary products derived from α-olefins. These authors advanced the view that growth of linear chains proceed at the same rate (α) for all species and that it is the termination event which is species specific. The break in the paraffin ASF plot is therefore caused by a sharp change in the rate of termination at about C_{13}. Since a number of investigators have found that the carbon number where the break occurs is about the same and since the break is observed with a variety of catalysts, they state that it may be that the phenomenon is governed by the nature of the C_{13} molecule as well as the catalyst.

Gaube and coworkers (IX.G-20,IX.G-21) also observed a two α plot. For an iron catalyst the C_3 - C_{40} products exhibit a linear ASF plot that only required a single α value (Figure IX.G-7). However, when the catalyst contained alkali (added as K_2CO_3), the ASF plot needed two α values to adequately describe the data. However, others have found the need for two alpha values for catalysts that do not contain potassium or other alkali metals (e.g., IX.G-22 - IX.G-25).

Donnelly et al. (IX.G-26) extended the chain growth theory to include two growth probabilities; thus, rather than equation [4] one should write

$$m_p = AP\alpha^P + BP\alpha^P \qquad [10]$$

The contribution of each growing chain will be equal at the break point. They offer this as an improved equation for analyzing FTS product distributions, and show that this equation adequately described their data.

Dictor and Bell (IX.G-22) found a two-alpha plot for both reduced and unreduced iron oxide catalysts. Furthermore, these authors found that the ASF plot for n-aldehydes yielded a two-alpha plot just as was the case for the hydrocarbon products. Furthermore, the break for the aldehydes was at the same carbon number as the hydrocarbons, provided the aldehyde ASF plot was based upon n-1 rather than n, as was used for the hydrocarbons (Figure IX.G-8). This was taken to support the view that aldehydes are formed by CO insertion into a growing surface alkyl group and subsequent reductive elimination of the acyl group (IX.G-27,IX.G-28); hydrocarbons on the other hand are believed to be formed in a termination step that occurs by elimination of a hydrogen from an alkyl group. Since the break occurs at n for hydrocarbons and n + 1 for the aldehydes, it appears that the oxygenate and hydrocarbon products are derived from a common surface species.

Donnelly and Satterfield (IX.G-24) utilized a Ruhrchemie catalysts in a CSTR and found that both the n-alkanes and 1-alkenes fit a two-alpha ASF plot (Figure IX.G-8) whereas earlier work from that laboratory (IX.G-18) showed that only n-alkanes deviated from ASF. In contrast to Dictor and Bell (IX.G-22), Donnelly and Satterfield (IX.G-24) found that oxygenates followed a single alpha plot even though they now find, in contrast to earlier results, that both n-alkanes and 1-alkenes deviate

from ASF. These data serve to illustrate the difficulty in deciding the one or two-alpha plot question.

Stenger (IX.G-29) showed that the two site ASF equation used by Huff and Satterfield was equivalent to one based on a distributed-site model in its ability to fit the molecular weight product distribution from an iron catalyst promoted with potassium. In the promoted catalyst, a distribution of sites proportional to the concentration of potassium relative to iron is utilized. In his model, Stenger assumed a normal distribution of K on the surface and postulated an exponential dependence of alpha on the random distribution variable, X, that is proportional to the potassium distribution.

Inoui et al. (IX.G-30) introduced a single criterion to differentiate between the two-site model (IX.G-24) and a distributed site model (IX.G-29). However, for typical values of α_1 and α_2 for iron catalysts ($\sim$0.6 and 0.8, respectively) the fit to the ASF plot should make it difficult to distinguish the two models, even using the approach suggested by Inoui et al.

Kikuchi and Itoh (IX.G-31) utilized an iron catalyst based upon ultrafine particles loaded with 1% K and found a break in the ASF plot at C_{10}. The data fit the model based upon two kinds of sites, A and B, with A exhibiting the lower and B exhibiting the higher growth probability. The fit of the experimental data and the calculated curve was satisfactory (Figure IX.G-9).

Iglesia et al. (IX.G-32) reported that olefins readsorb and initiate surface chains that are indistinguishable from those formed directly from CO/H_2. Diffusion enhanced olefin readsorption leads to an increase in chain growth probability, α, and in paraffin

content with increasing pore and bed residence time. Deviations from conventional (ASF) polymerization kinetics were quantitatively described by transport effects on the residence time of intermediate olefins within the liquid-filled catalyst pores without requiring the presence of several types of chain growth sites. The results reported for this study were obtained with a Ru catalyst, and not an iron catalyst.

Not all of the earlier studies require two or more α values to describe the distribution of products from FTS with iron catalysts. Three examples of this will be noted. Zwart and Vink (IX.G-33) report that the product from zeolite supported iron catalysts derived from iron carbonyl complexes produced a product distribution in the C_{3-20} range which obeyed ASF statistics in all cases. Eilers et al. (IX.G-34) report that in a few hundred independent FTS experiments with various catalyst formulations under different operating conditions it was confirmed that the carbon number distribution were in close agreement with the ASF kinetics (Figure IX.G-10). However, neither of the two data sets for the iron catalysts cover the total range of carbon numbers where the break in the ASF plot is observed. Cannella (IX.G-35) reported a linear ASF plot that only required one alpha value to fit the C_{3+} products for an unsupported iron catalyst but that a two-alpha plot was required for the K-promoted catalyst. Linear ASF plots were always obtained for the C_3^+ products produced over each of the supported iron catalysts.

Tau et al. (IX.G-36) found that a doubly promoted C-73 catalyst incorporated ^{14}C labeled 1-pentanol, added to the CO/H_2 feed, into higher carbon number products. They found that product accumulation in the CSTR was not adequate to

explain the deviation from a constant ^{14}C activity/mole with increasing carbon number for higher carbon number alkane products.

^{14}C labeled ethanol served only as a chain initiator; this is demonstrated by the constant ^{14}C activity/mole for the C_2 through C_4 products (Figure IX.G-11). The constant activity of C_3 and C_4 that is equal to ethanol indicates that only one C_2 species derived from ethanol was incorporated into these products. These results are in agreement with the earlier data obtained by Emmett and coworkers (IX.G-15, IX.G-37 - IX.G-41).

However, the data in Figure IX.G-12 clearly indicate that the C_{10} - C_{14} paraffins exhibit a different ^{14}C activity pattern with increasing carbon number than those in the C_2 - C_4 range. The higher carbon number products are diluted by the products accumulated in the reactor prior to the addition of ^{14}C labeled 1-pentanol. Analysis of the wax withdrawn from the reactor prior to the addition of the ^{14}C tracer provided data to calculate the impact of these products in diluting the ^{14}C content of higher carbon number products. Dilution did provide a minor contribution to the negative slope of the ASF plot in Figure IX.G-12; however, the points corrected for accumulation (◆) provided only a modest correction toward that exhibited by the lower carbon number products where ^{14}C/mole was constant with increasing carbon number (Figure IX.G-11). Hence, the effect of accumulation alone cannot account for the experimental data.

Another explanation for the deviation from the ASF plot is that hydrogenolysis of higher carbon number compounds produce more lower carbon number hydrocarbon products than can be accounted for by ASF. Using the same C-73

catalyst, Huang et al. (IX.G-42) used octacosane, labeled at the carbon-14 position of the chain, to show that a detectable amount of hydrogenolysis did not occur even after one week of operation at the same conditions as was used by Tau et al. (IX.G-36). Thus, hydrogenolysis is eliminated as an explanation for the two-alpha ASF plot for a promoted iron catalyst.

Tau et al. (IX.G-36) concluded that the two alpha values in Figure IX.G-4 correspond to different product groupings. For the smaller alpha (about 0.62) the typical Fischer-Tropsch products are formed (alkanes, alkenes, oxygenates, etc.). However, for the larger alpha (about 0.82) the only significant product obtained corresponds to alkanes. The data in Figure IX.G-13, after first correcting for accumulation and then for the two different product groups, show a constant ^{14}C/mole, causing the conclusion based upon the higher carbon alkane products to be consistent with the one based on the lower alkane products.

In conclusion, it is evident that many groups using a variety of iron catalysts have found that two or more alpha values are needed if ASF kinetics are to account for the FTS products. The summary of the two-alpha values (IX.G-43) for eight studies emphasize this conclusion. It is possible for deficiencies in the analytical determinations or loss of certain carbon number ranges during sampling or testing could cause the break in the ASF plot. However, this is not possible for the ^{14}C studies since the conclusion is based upon the ^{14}C/mole rather than the total number of moles. Recent data using ^{14}C-ethanol (IX.G-44) and analysis of a wider carbon number range than in reference IX.G-36 provide additional support for the results reported by Tau et al. Furthermore, similar results are obtained for the addition of ^{14}C

labeled C_2, C_3, C_5, C_6 and C_{10} alcohols and C_2, C_5 and C_{10} alkenes (IX.G-45,IX.G-46). With emphasis on the ^{14}C tracer studies, we conclude that it is likely that at least two chains are growing independently, and that these independent chains lead to different groups of products. These in turn require at least two-alpha values for the ASF to adequately describe the FTS data.

As shown in Section IX.E, the aging of a catalyst can introduce an apparent two-alpha curve even though the data represents a single alpha case. We are continuing to work on developing a better method for the calculation of the value(s) of alpha as well as the reliability of both the alpha value(s) and the fraction of the product that each alpha chain growth process contributes to the yield. The ability to analyze hydrocarbons to carbon numbers of about 100 will allow us to measure an alpha for the reactor wax and to test how this alpha compares with the second alpha calculated from the lower carbon number hydrocarbons.

REFERENCES

IX.G-1. H. Kölbel and M. Ralek, *Catal. Rev.-Sci. Eng.*, **21**, 225 (1980).

IX.G-2. H. Kölbel, P. Ackermann and Fr. Engelhardt, *Erdöl Kohle*, **9**, 225 (1956).

IX.G-3. J. C. W. Kuo, Slurry Fischer-Tropsch/Mobil two stage process of converting syngas to high octane gasoline; DOE/PC/30022-10, June 1983.

IX.G-4. L.-M. Tau, H. A. Dabbagh and B. H. Davis, *Energy & Fuels*, **4**, 719 (1990).

IX.G-5. G. V. Schulz, *Z. Phys. Chem.*, **29**, 299 (1935); **30**, 375 (1935).

IX.G-6. G. V. Schulz, *Z. Phys. Chem.*, **30**, 375 (1936).

IX.G-7. P. J. Flory, *J. Amer. Chem. Soc.*, **58**, 1877 (1936).

IX.G-8. E. F. G. Herrington, *Chem. Ind.*, (1946) 347.

IX.G-9. R. A. Friedel and R. B. Anderson, *J. Amer. Chem. Soc.*, **72**, 1212 (1950); **72**, 2307 (1950).

IX.G-10. S. Weller and R. A. Friedel, *J. Chem. Phys.*, **17**, 801 (1949).

IX.G-11. R. B. Anderson, "The Fischer-Trospch Synthesis", Academic Press, New York, 1984.

IX.G-12. R. B. Anderson in "Catalysis" (P.H. Emmett, ed.) Reinhold Pub. Corp., New York, 1956, Vol. IV, pp 22-256.

IX.G-13. R. J. Madon and W. F. Taylor, *J. Catal.*, **69**, 32 (1981).

IX.G-14. J. F. Schulz, W. K. Hall, B. Seligmon and R. B. Anderson, *J. Amer. Chem. Soc.*, **77**, 211 (1955).

IX.G-15. W. K. Hall, R. J. Kokes and P. H. Emmett, *J. Amer. Chem. Soc.*, **82**, 1027 (1960).

IX.G-16. S. Novak, R. J. Madon and H. Suhl, *J. Catal.*, **77**, 141 (1982).

IX.G-17. C. N. Satterfield and G. A. Huff, Jr., *J. Catal.*, **73**, 187 (1982).

IX.G-18. G. A. Huff, Jr. and C. N. Satterfield, *J. Catal.*, **85**, 370 (1984).

IX.G-19. N. O. Egiebor, W. C. Cooper and B. W. Wojciechowski, *Canadian J. Chem. Eng.*, **63**, 826 (1985).

IX.G-20. L. Konig and J. Gaube, *Chem. Ing. Tech.*, **55**, 14 (1983).

IX.G-21. B. Schliebs and J. Gaube, *Ber. Bunsenges. Phys. Chem.*, **39**, 68 (1985).

IX.G-22. R. A. Dictor and A. T. Bell, *J. Catal.*, **97**, 121 (1986).

IX.G-23. L.-M. Tau, H. Dabbagh, B. Chawla and B. H. Davis, "Mechanism of Promotion of Fischer-Tropsch Catalysts", DOE/PC/70029-T1, Final Report, December 1987.

IX.G-24. T. J. Donnelly and C. T. Satterfield, *Appl. Catal.*, **52**, 93 (1989).

IX.G-25. H. Itoh, H. Hosaka and E. Kikuchi, *Appl. Catal.*, **40**, 53 (1988).

IX.G-26. T. J. Donnelly, I. C. Yates and C. N. Satterfield, *Energy & Fuels*, **2**, 734 (1988).

IX.G-27. H. Schulz and A. Zein El Deen, *Fuel Proc. Tech.*, **1**, 45 (1977).

IX.G-28. P. Biloen, J. N. Helle and W. M. H. Sachtler, *J. Catal.*, **58**, 95 (1979).

IX.G-29. H. G. Stenger, Jr., *J. Catal.*, **92**, 426 (1985).

IX.G-30. M. Inoui, T. Miyake and T. Inui, *J. Catal.*, **105**, 266 (1987).

IX.G-31. E. Kikuchi and H. Itoh, "Methane Conversion" (D. M. Bibby et al., eds.) Elsevier Sci. Pub., Amsterdam, 1988, pp 517-521.

IX.G-32. E. Iglesia, S. C. Reyes and R. J. Madon, "Transport-Enhanced Olefin Readsorption Model of Hydrocarbon Synthesis Selectivity", 12th NAM of The Catalysis society, Abstract PC02, Lexington, KY, May 5-9, 1991.

IX.G-33. J. Zwart and J. Vink, *Appl. Catal.*, **33**, 383 (1987).

IX.G-34. J. Eilers, S. A. Posthuma and S. T. Sie, *Catal. Lett.*, **7**, 253 (1990).

IX.G-35. W. J. Cannella, Ph.D. dissertation, U. of California, Berkeley, 1984.

IX.G-36. L.-M. Tau, H. Dabbagh, S.-Q. Bao and B. H. Davis, *Catal. Lett.*, **7**, 127 (1990).

IX.G-37. W. K. Hall, R. J. Kokes and P. H. Emmett, *J. Amer. Chem. Soc.*, **79**, 2983 (1957).

IX.G-38. J. T. Kummer, T. W. DeWitt and P. H. Emmett, *J. Amer. Chem. Soc.*, **70**, 3632 (1948).

IX.G-39. J. T. Kummer and P. H. Emmett, *J. Amer. Chem. Soc.*, **75**, 5177 (1953).

IX.G-40. J. T. Kummer, H. H. Podgurski, W. B. Spencer and P. H. Emmett, *J. Amer. Chem. Soc.*, **73**, 564 (1951).

IX.G-41. G. Blyholder and P. H. Emmett, *J. Phys. Chem.*, **63**, 962 (1959); **62**, 470 (1960).

IX.G-42. C. S. Huang, H. Dabbagh and B. H. Davis, *Appl. Catal.*, **73**, 237 (1991).

IX.G-43. D. K. Matsumoto and C. N. Satterfield, *Energy & Fuels*, **3**, 249 (1989).

IX.G-44. Unpublished data.

IX.G-45. L.-M. Tau, H. A. Dabbagh and B. H. Davis, *Energy & Fuels*, **5**, 174 (1991).

IX.G-46. L.-M. Tau, H. A. Dabbagh and B. H. Davis, *Enertgy & Fuels*, **4**, 94 (1990).

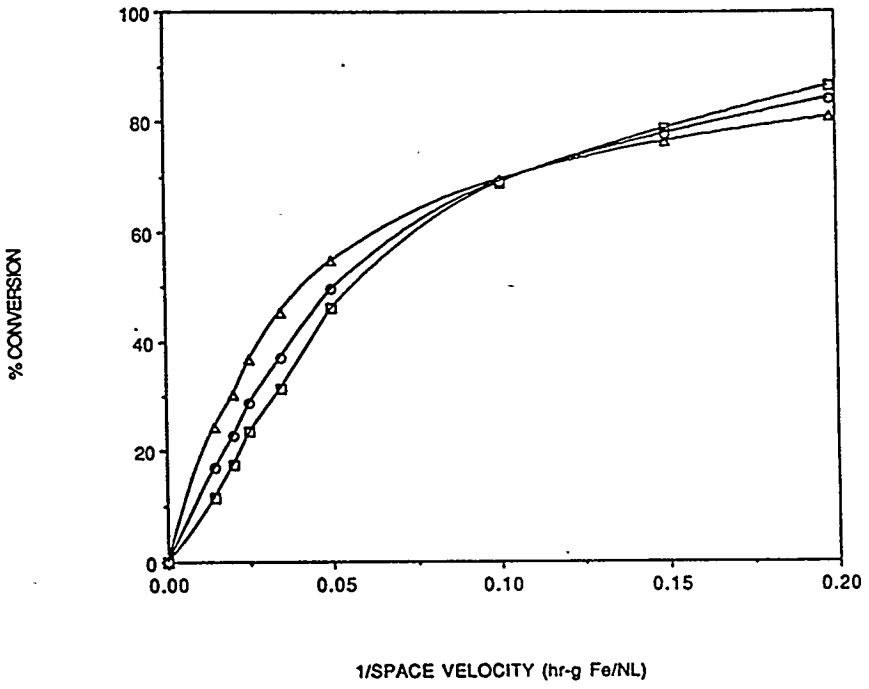

Figure IX.G-1. The conversion of CO (□), H_2 (△) on synthesis gas (H_2/CO = 0.7) (○) as a function of the inverse of the space velocity (270°C, 12.9 atm., 100 Fe/4.4 Si/0.71 K).

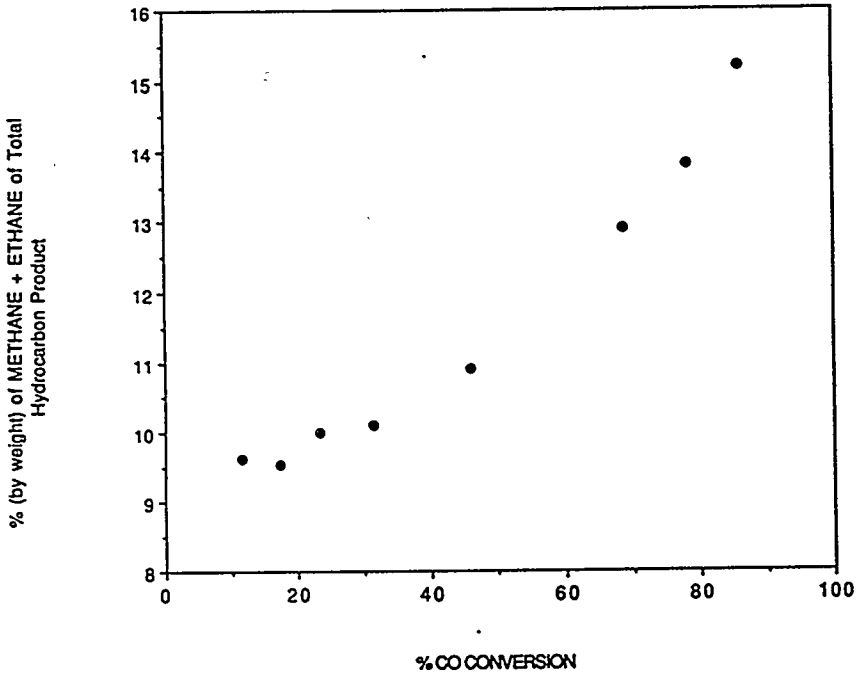

Figure IX.G-2. Dependence on methane plus ethane, as percentage of total hydrocarbons, upon the total CO conversion (270°C, 12.9 atm., H122/CO = 0.7, and various space velocities).

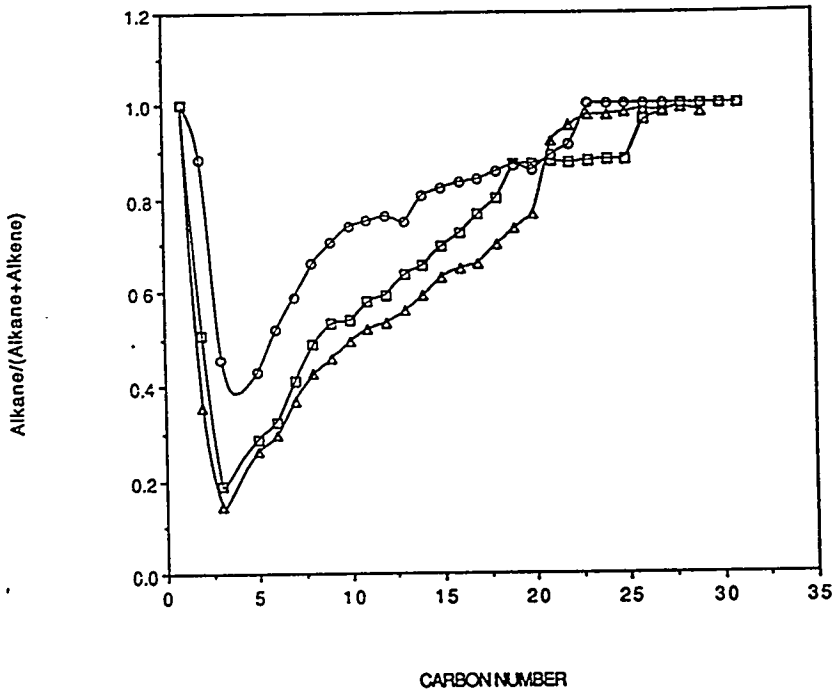

Figure IX.G-3. Dependence of alkane fraction [alkane (1- + c-2- + trans-2-alkene + alkane)] on the carbon number (conversion = 16% (△), 49% (□) and 85% (○); reaction conditions as in figure IX.G-1.

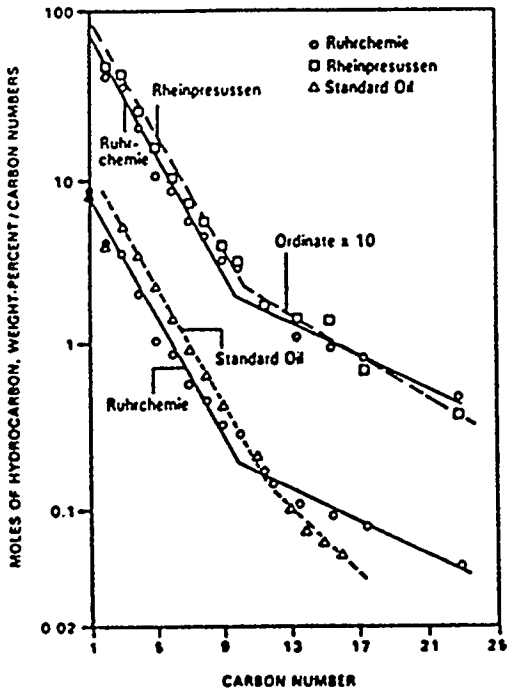

Figure IX.G-4. Anderson-Schulz-Flory (ASF) plots for the products from Schwarzheide for catalysts for four sources and Standard Oil Company of New Jersey (reproduced from ref. IX.G-12, p. 208).

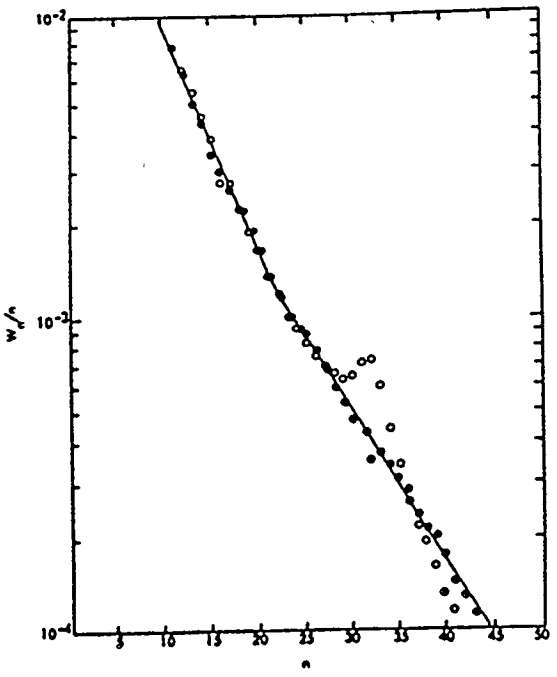

Figure IX.G-5. Plot of ln W_n/n versus carbon number n. Open points, unsulfided catalysts; solid points, sulfided catalyst (reproduced from ref. IX.G-13.

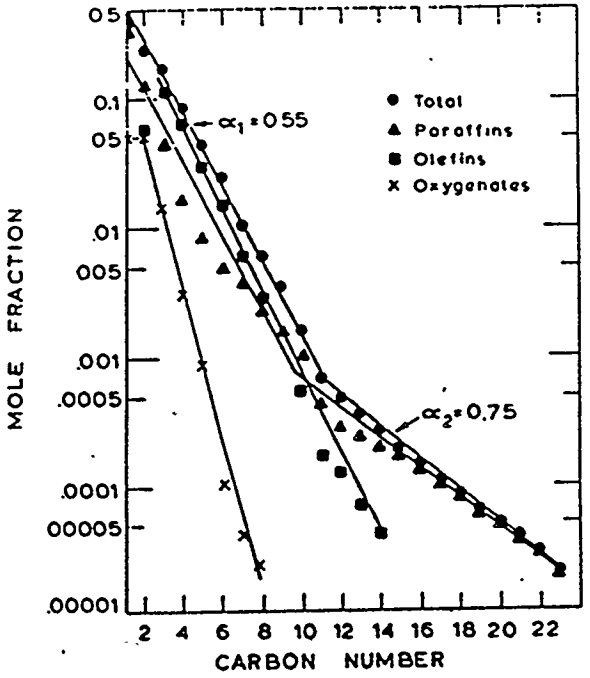

Figure IX.G-6. Flory distribution of MnO/Fe catalyst; 283°C, 1.24 MPa, $(H_2/CO)_m$ = 1.19 (reproduced from ref. IX.G-18).

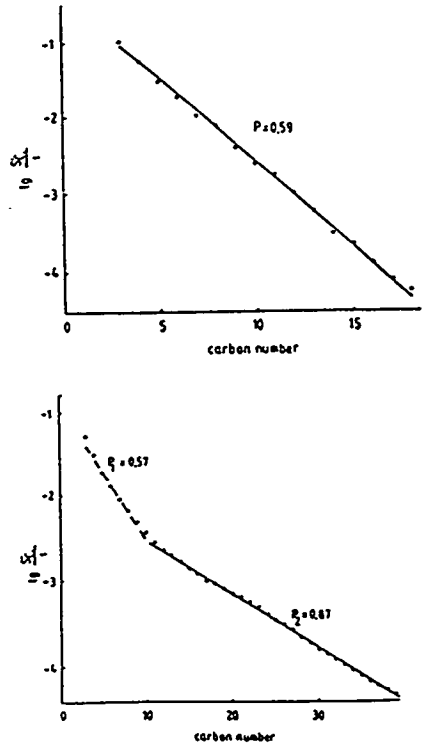

Figure IX.G-7. Product distribution from FTS using an iron (top) and potassium promoted iron catalyst (bottom) (redrawn from ref. IX.G-20).

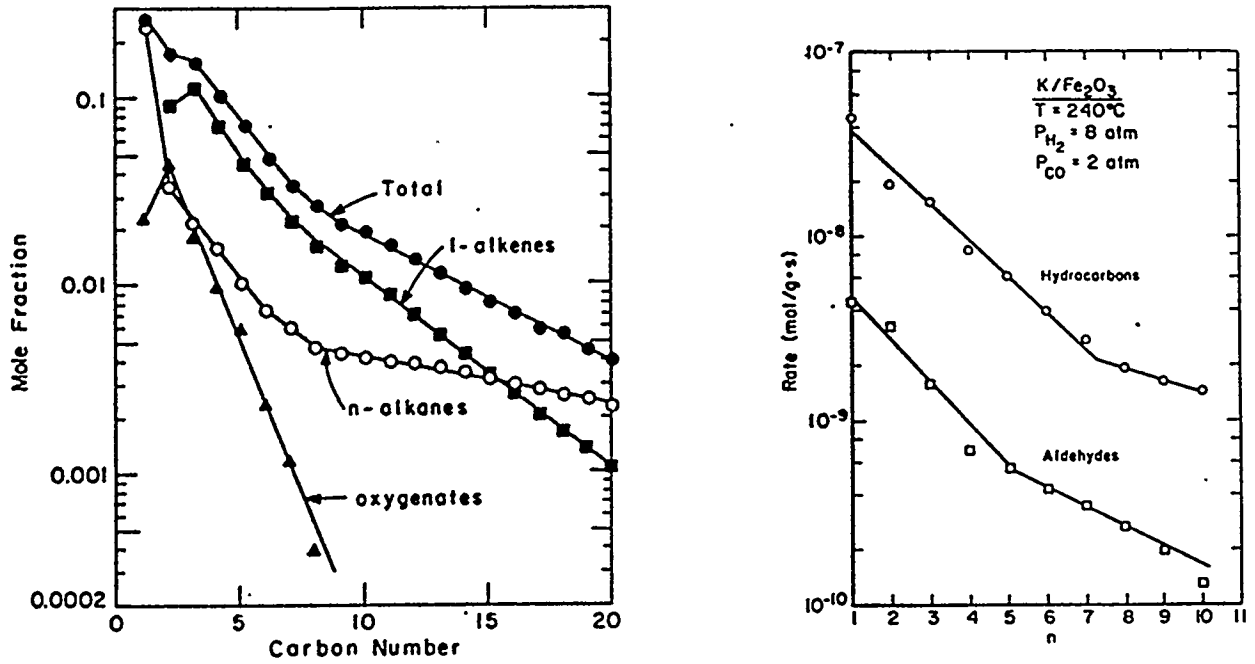

Figure IX.G-8. (left) Component Schulz-Flory diagram for overhead products. Ruhrchemie Catalyst MPa, 0.034 Nl/min/g_{cat}, $(H_2/CO)_{feed}$ = 0.7, 600 hours-on-stream (reproduced from ref. IX.G-24). (right) Distribution of hydrocarbons and aldehydes from a common effluent sample. Each point for hydrocarbons represents the sum of 1-olefin plus n-paraffin; only straight-chain aldehydes are measured (reproduced from ref. IX.G-22).

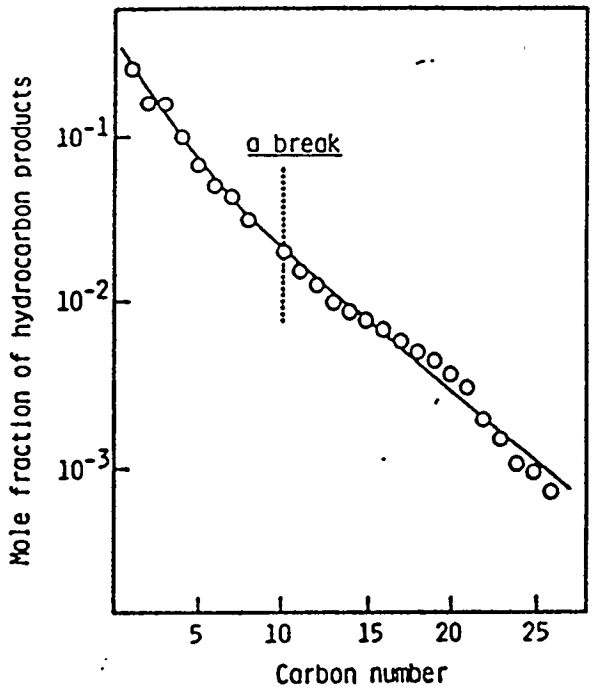

Figure IX.G-9. Flory plot of hydrocarbon products over potassium-promoted Fe UFP (ultrafine particle) catalyst. Reaction conditions: temperature, 220°C; pressure, 30 atm; H_2/CO, 1 mol/mol; W/F, 300 g-cat.min/CO-mol. Potassium addition: 1 wt.% of catalyst. Solid line represents the simulated distribution based on two-site ASF equation (reproduced from ref. IX.G-25).

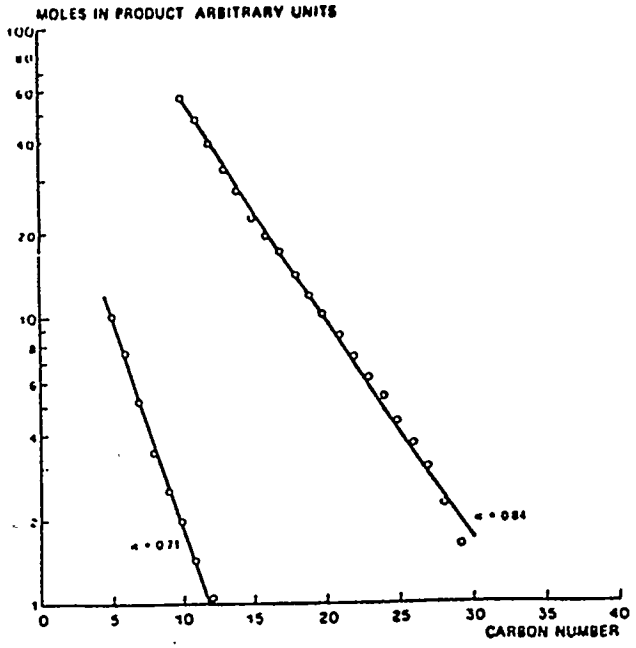

Figure IX.G-10. Typical carbon number distribution of the FTS using an iron catalyst (redrawn from ref. IX.G-34).

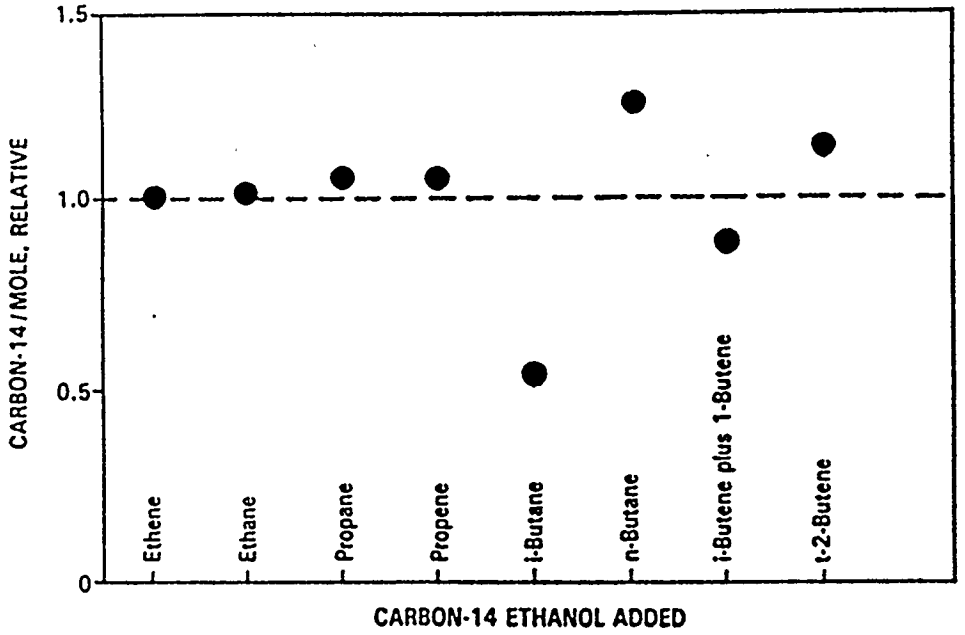

Figure IX.G-11. Relative ^{14}C/mole in gaseous products from the synthesis (7 atm, $H_2/CO = 1.2$, 262°C) with 3-volume % (based on alcohol and CO) [^{14}C-1]-ethanol was added during a 24 hour period (redrawn from ref. IX.G-36).

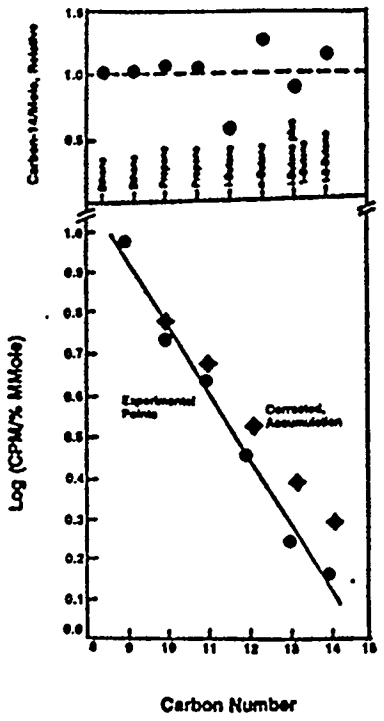

Figure IX.G-12. Composite figure showing relative radioactivity for the lower carbon number compounds (●); the measured values for the higher carbon number compounds (◆), and the values for the higher carbon number compounds (■) after correcting for reactor accumulation effects (redrawn from IX.G-45).

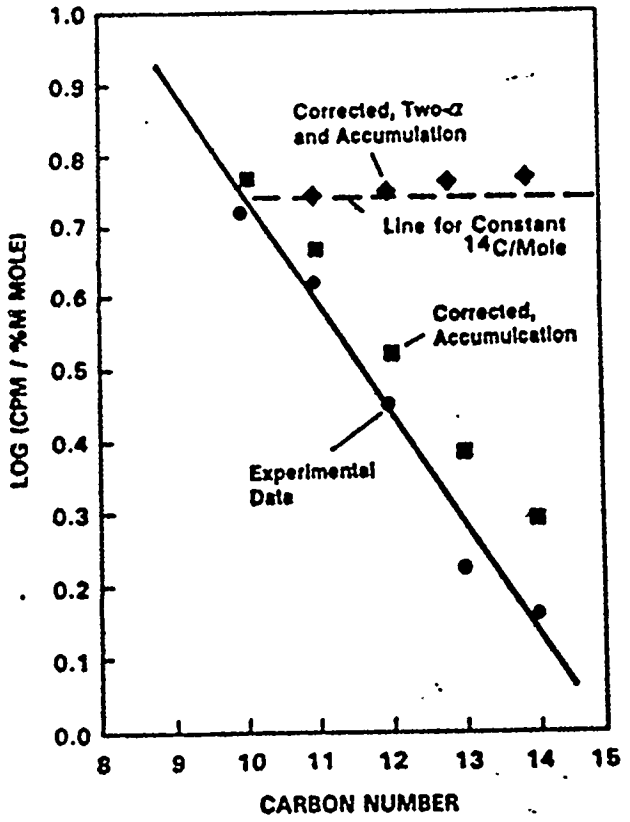

Figure IX.G-13. Radioactivity of the: alkane products (●); experimental data corrected for accumulation using data shown in Table 1 (■), and experimental data corrected for both accumulation and the two alpha mechanism (see text for details) (◆) (redrawn from ref. IX.G-45).